Metabolic Engineering Communications 3 (2016) 68–75

Contents lists available at ScienceDirect

Metabolic Engineering Communications

journal homepage: www.elsevier.com/locate/mec

Mitochondrial targeting increases specific activity of a heterologous valine assimilation pathway in *Saccharomyces cerevisiae*

Kevin V. Solomon [a,1], Elisa Ovadia [a,2], Fujio Yu [b], Wataru Mizunashi [b], Michelle A. O'Malley [a,*]

[a] Department of Chemical Engineering, University of California Santa Barbara, Santa Barbara, CA 93106, United States
[b] Science and Technology Research Center, Inc., Mitsubishi Rayon Group, Yokohama, Kanagawa 227-8502, Japan

ARTICLE INFO

Article history:
Received 7 February 2016
Accepted 14 March 2016
Available online 15 March 2016

Keywords:
Pseudomonas
Isobutanol
Dehydrogenase
Mitochondria
Saccharomyces cerevisiae
Metabolic engineering

ABSTRACT

Bio-based isobutantol is a sustainable 'drop in' substitute for petroleum-based fuels. However, well-studied production routes, such as the Ehrlich pathway, have yet to be commercialized despite more than a century of research. The more versatile bacterial valine catabolism may be a competitive alternate route producing not only an isobutanol precursor but several carboxylic acids with applications as biomonomers, and building blocks for other advanced biofuels. Here, we transfer the first two committed steps of the pathway from pathogenic *Pseudomonas aeruginosa* PAO1 to yeast to evaluate their activity in a safer model organism. Genes encoding the heteroligomeric branched chain keto-acid dehydrogenase (BCKAD; *bkdA1, bkdA2, bkdB, lpdV*), and the homooligomeric acyl-CoA dehydrogenase (ACD; *acd1*) were tagged with fluorescence epitopes and targeted for expression in either the mitochondria or cytoplasm of *S. cerevisiae*. We verified the localization of our constructs with confocal fluorescence microscopy before measuring the activity of tag-free constructs. Despite reduced heterologous expression of mitochondria-targeted enzymes, their specific activities were significantly improved with total enzyme activities up to 138% greater than those of enzymes expressed in the cytoplasm. In total, our results demonstrate that the choice of protein localization in yeast has significant impact on heterologous activity, and suggests a new path forward for isobutanol production.

1. Introduction

Yeast microbial factories for biochemical production are competitive alternatives to bacterial platforms. As simple eukaryotes, yeast offer wider product portfolios (Adrio and Demain, 2010; Demain and Vaishnav, 2009) and improved tolerance to toxic value-added products (Ingram, 1986), while remaining relatively simple to engineer. These improved capabilities arise from their ability to compartmentalize their metabolic functions. By spatially separating reactions in this manner, eukaryotes locally concentrate precursors and enzymes where they are needed (Fukuda et al., 2005; Kumar et al., 2002; Paltauf et al., 1992), enhancing the efficiency of these processes. Compartmentalization also establishes fixed environmental conditions (e.g. pH (Orij et al., 2009) and redox potential (Hu et al., 2008)), which affect the enzyme kinetics and potential chemistries within them. For instance, disulfide bond formation is thermodynamically favored in the oxidizing environment of the endoplasmic reticulum (Woycechowsky and Raines, 2000), while the substantial pH gradient across the mitochondrial membrane drives ATP biosynthesis (Mitchell, 1961). The thermodynamic and kinetic advantages offered by these environments, however, have historically been ignored in engineering applications due to the increased complexity of eukaryote biology and the poorly defined nature of many localization signal sequences (Kim and Hwang, 2013).

The resurgent interest in the Ehrlich pathway for the production of advanced 'drop-in' biofuels such as isobutanol (Avalos et al., 2013; Branduardi et al., 2013; Smith and Liao, 2011) has led to innovative strategies for pathway design. One of the most promising leverages the improved tolerance of yeast, and their ability to localize key heterologous enzymes to the mitochondria where they have ready access to needed precursors (Avalos et al., 2013). In comparison to traditional cytosolic expression, yields of isobutanol were improved by more than 2-fold due to the increased local concentration of precursors and enzymes in the compartment's reduced volume (Avalos et al., 2013). Despite

* Corresponding author.
E-mail address: momalley@engineering.ucsb.edu (M.A. O'Malley).
[1] Present address: Agricultural & Biological Engineering, Purdue University, West Lafayette, IN 47907, United States.
[2] Present address: Chemical and Biomolecular Engineering, University of Delaware, Newark, DE 19716, United States.

http://dx.doi.org/10.1016/j.meteno.2016.03.004

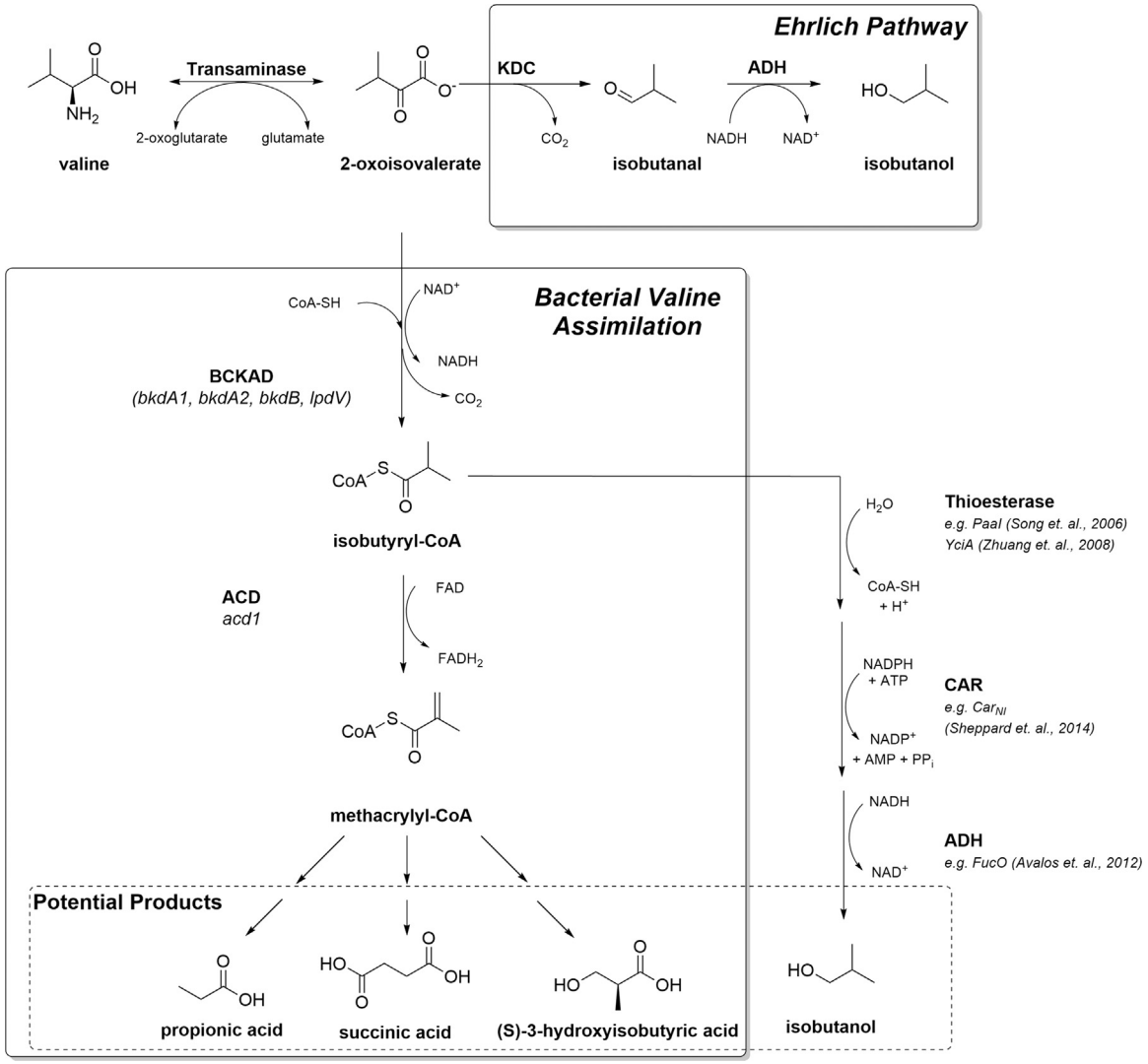

Fig. 1. Valine Assimilation Pathways and Potential Products. Ehrlich (Hazelwood et al., 2008) and bacterial valine assimilation (Massey et al., 1976) routes to isobutanol (Avalos et al., 2013; Sheppard et al., 2014; Song et al., 2006; Zhuang et al., 2008), biomonomers, and fuel building blocks. Genes for ACD and BCKAD from *P. aeruginosa* are italicized. ACD – Acyl-CoA dehydrogenase; ADH – alcohol dehydrogenase; BCKAD – branched chain keto-acid dehydrogenase; CAR – carboxylic acid reductase; KDC – keto-acid decarboxylase.

these successes, the titers were insufficient for commercialization and future efforts may benefit from alternate metabolic routes to product. More importantly, however, the impact of the compartment's environment on heterologous activity remains unexamined.

A promising alternate route to isobutanol is through the bacterial valine assimilation pathway (Fig. 1). Bacterial catabolism oxidatively decarboxylates α-keto acids to acyl-CoAs that may be cleaved with a thioesterase and reduced to release fusel alcohols (Sheppard et al., 2014). Extensions of the native pathway also produce a number of other valuable products such as biomonomers, and fatty alcohols (Massey et al., 1976). To evaluate the commercial potential of this pathway, we first examined the feasibility of heterologous expression of these enzymes in more fuel-tolerant non-pathogenic yeast. We cloned and expressed the oxidative decarboxylase, branched chain keto-acid dehydrogenase (BCKAD), and the subsequent oxidase of the native pathway, acyl-CoA dehydrogenase (ACD), from *Pseudomonas aeruginosa* PAO1. These enzymes were targeted for expression in either the mitochondria or cytoplasm of *S. cerevisiae* in a multi-plasmid/multigene background to recreate the metabolic burden of a complete production pathway. Here, we quantify their recombinant activity and examine the effects of enzyme localization on specific activity.

2. Materials and methods

2.1. Strains and plasmids

S. cerevisiae and *E. coli* strains and plasmids used in this study are listed in Table 1. Sub-cloning was carried out according to standard practices (Sambrook and Russell, 2001) and plasmids were maintained in *E. coli* XL1B. *acd1* (PA0746), *bkdA1* (PA2247), *bkdA2* (PA2248), *bkdB* (PA2249), and *lpdV* (PA2250), encoding the acyl-CoA dehydrogenase and branched chain keto acid dehydrogenase complex, respectively, from *Pseudomonas aeruginosa* PA01, were PCR amplified from plasmid template (pMMA202) provided by Mitsubishi Rayon. These amplicons were cloned into the BglII sites of the galactose-inducible pYES-mtGFP vector, graciously provided by Prof. Dr. Westermann, Universität Bayreuth, Germany, with the primers listed in Table 2. These constructs target expression of a C-terminal gene-Green Fluorescent Protein (GFP) fusion to the mitochondria via the included mitochondrial (*mt*) leader peptide

Table 1
Strains and plasmids.

Name	Relevant genotype	Vector backbone	Plasmid type	Source
***E. coli* strains**				
XL1B	*endA1 gyrA96(nal^R) thi-1 recA1 relA1 lac glnV44 F'[::Tn10 proAB$^+$ lacI^q Δ(lacZ)M15] hsdR17($r_K^-m_K^+$)*			Stratagene (Santa Clara, CA)
***S. cerevisiae* strains**				
CKY263	*MATa leu2-3, 112 ura3-52 GAL*			(Frand and Kaiser, 1999)
BJ5464	*MATα ura3-52 trp1 leu2Δ1 his3 Δ 200 pep4::HIS3 prb1Δ1.6R can1 GAL*			(Jones, 1991)
Plasmids				
pYESmtGFP	YEp *bla* pBR322 URA3 GAL1-*mtGFP*-CYCT	pYES	2μ	(Westermann and Neupert, 2000)
pRS316-PP-Pfu_blgA	YEp *bla* pBR322 URA3 GAL1 Prepro-*bglA*-His_{10} CYCT	pRS316	2μ	This study
pYES-acd-GFP	YEp *bla* pBR322 URA3 GAL1-*acd1-GFP*-CYCT	pYES	2μ	This study
pYES-mtacd-GFP	YEp *bla* pBR322 URA3 GAL1-*mtacd1-GFP*-CYCT	pYES	2μ	This study
pYES-acd	YEp *bla* pBR322 URA3 GAL1-*acd1*-CYCT	pYES	2μ	This study
pYES-mtacd	YEp *bla* pBR322 URA3 GAL1-*mtacd1*-CYCT	pYES	2μ	This study
pYES-bkdA1-GFP	YEp *bla* pBR322 URA3 GAL1-*bkdA1-GFP*-CYCT	pYES	2μ	This study
pYES-mtbkdA1-GFP	YEp *bla* pBR322 URA3 GAL1-*mtbkdA1-GFP*-CYCT	pYES	2μ	This study
pYES-bkdA2-GFP	YEp *bla* pBR322 URA3 GAL1-*bkdA2-GFP*-CYCT	pYES	2μ	This study
pYES-mtbkdA2-GFP	YEp *bla* pBR322 URA3 GAL1-*mtbkdA2-GFP*-CYCT	pYES	2μ	This study
pYES-bkdB-GFP	YEp *bla* pBR322 URA3 GAL1-*bkdB-GFP*-CYCT	pYES	2μ	This study
pYES-mtbkdB-GFP	YEp *bla* pBR322 URA3 GAL1-*mtbkdB-GFP*-CYCT	pYES	2μ	This study
pYES-lpdV-GFP	YEp *bla* pBR322 URA3 GAL1-*lpdV-GFP*-CYCT	pYES	2μ	This study
pYES-mtlpdV-GFP	YEp *bla* pBR322 URA3 GAL1-*mtlpdV-GFP*-CYCT	pYES	2μ	This study
pACD1	YEp *bla* pBR322 URA3 GAL1-*acd1*-CYCT	pRS316	2μ	This study
pmtACD1	YEp *bla* pBR322 URA3 GAL1-*mtacd1*-CYCT	pRS316	2μ	This study
pBCKAD4	YEp *bla* pBR322 LEU2 GAL1-*bkdA1*-CYCT GAL1-*bkdA2*-CYCT GAL1-*bkdB*-CYCT GAL1-*lpdV*-CYCT	pRS315	2μ	This study
pmtBCKAD4	YEp *bla* pBR322 LEU2 GAL1-*mtbkdA1*-CYCT GAL1-*mtbkdA2*-CYCT GAL1-*mtbkdB*-CYCT GAL1-*mtlpdV*-CYCT	pRS315	2μ	This study
pCoA2	YEp *bla* pBR322 LEU2 GAL1-*hchA*-CYCT GAL1-*echA3*-CYCT	pRS314	2μ	This study
pmtCoA2	YEp *bla* pBR322 LEU2 GAL1-*mthchA*-CYCT GAL1-*mtechA3*-CYCT	pRS314	2μ	This study

Table 2
Primers used.

Gene	Forward (5′→3′)	Reverse (5′→3′)
acd1	CTAT**AGATCT**AAGCTTATGGATTTCGACCTCACC	CTAT**AGATCT**CAGCAGGCGATCGAG
bkdA1	CTAT**AGATCT**AAGCTTATGAGTGATTACGAGCCGT	CTAT**AGATCT**TACCCCGAGCTCCTG
bkdA2	CTAT**AGATCT**AAGCTTATGAATGCCATGAACCC	CTAT**AGATCT**GACCTCCATCACACGCT
bkdB	CTAT**AGATCT**AAGCTTATGGGTACCCATGTGATCA	CTAT**AGATCT**CTCCAGGAACAGGGTGG
lpdV	CTAT**AGATCT**AAGCTTATGAGCCAGATCCTGAAGAC	CTAT**AGATCT**GATGTGCAGGGCGTG
hchA	CTAT**AGATCT**AAGCTTATGAACGTGCTTTTCGAAG	CTAT***GAATTC***TCATCAGAGCCCCGCC
echA3	CTAT**AGATCT**AAGCTTATGAACACTGCCGTCGAAC	CTAT***GAATTC***TCATCAGCAGTTGCGCCAC

Bolded sequence indicates introduced BglII restriction sites. Underlined sequence indicates introduced HindIII sites. Bold italicized sequences indicate an introduced EcoRI restriction site.

sequence (Westermann and Neupert, 2000). To simulate the metabolic burden of carboxylic acid production, *echA3*(PA0745) and *hchA*(PA0744) encoding enoyl-CoA hydratases were cloned between the BglII and EcoRI sites of pYES-mtGFP with the primers in Table 2 to target expression to the mitochondria via the included *mt* leader peptide sequence and fluorescence epitope (Westermann and Neupert, 2000). Cytoplasmic expression was achieved by removing the *mt* leader sequence in these plasmids by cleaving with HindIII and circularizing the resulting product. As a fluorescent negative control, a beta-glucosidase construct from *Pyrococcus furiosus* (prepro-BglA-His_{10}) was cloned into pRS316 from pITY—PP—Pfu_bglA (O'Malley et al., 2012) via the flanking KpnI and SacI sites.

To reconstitute functional enzyme complexes and test activity, genes encoding heterologous enzymes were cloned together into a single plasmid using an idempotent cloning strategy inspired by the BioBrick standard (Fig. 2) (Knight, 2003). First, gene cassettes were amplified from the pYES series of vectors using universal primers 5pYES (5′-GATGATCCACTAGTACGGATTAG-3′) and 3Cyct (5′-CTAT**CCTAGG**TGCAGGGCCGC-3′) containing a native SpeI site (underlined) and an introduced AvrII site (bold). The amplicons generated with these primers lack the C-terminal GFP tag to preclude any issues with oligomerization and activity. These sites produce compatible cohesive ends (CTAG), which allow for the sequential addition of gene cassettes using the same restriction enzymes without the loss of previously integrated cassettes. (mt) *acd1* was cloned into pRS316 to make p(mt)ACD1, (mt)*bkdA1*, (mt) *bkdA2,* (mt)*bkdB,* and (mt)*lpdV* were cloned into pRS315 to make p (mt)BCKAD4, while (mt)*echA3* and (mt)*hchA* were cloned into pRS314 to make p(mt)CoA2. This cloning strategy generated 3 enzyme 'modules' (oxidative decarboxylation – p(mt)BCKAD4, subsequent reduction – p(mt)ACD1, and thioester cleavage to carboxylic acids via the hydratases – p(mt)CoA2) targeted to either the mitochondria or cytoplasm for 6 plasmids in total (Fig. 2).

Unless otherwise noted, PCR amplifications were performed with Phusion High-Fidelity DNA Polymerase (NEB, Ipswich, MA) and oligonucleotides synthesized by Eurofins Genomics (Huntsville, AL).

2.2. Culture conditions

Constructed plasmids were expressed in haploid *S. cerevisiae* strains CKY263 and BJ5464 after transformation using standard LiAc chemical transformation methods (Daniel Gietz and Woods, 2002). Bacterial strains were propagated on Luria-Bertani (LB) medium at 37 °C supplemented with 100 μg/ml ampicillin.

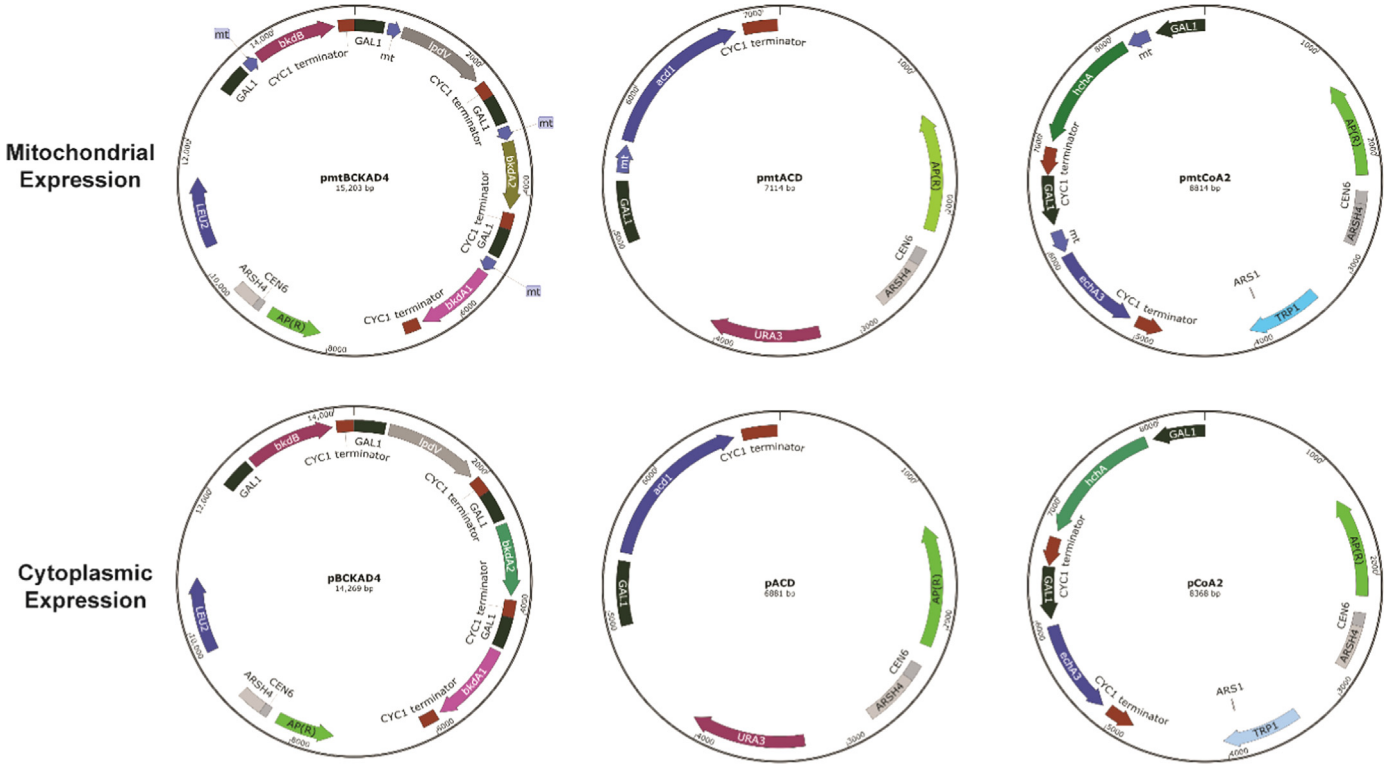

Fig. 2. Modular enzyme expression constructs. Gene subunits of each enzyme module are expressed together from a single galactose inducible plasmid. These plasmids target expression to either the cytoplasm or mitochondria (as indicated above) and contain compatible auxotrophic markers for co-expression as shown.

Initially, yeast strains were revived on glucose-rich YPD media before being transferred to either synthetic complete medium (SD-CAA) with the appropriate auxotrophic markers dropped out (Sherman, 2002), and supplemented with either 2% glucose or galactose. Cultures were induced on galactose at an OD of ~0.1 and expressed for at least 7 h before assaying their activity.

2.3. Protein localization

S. cerevisiae CKY263 cultures were propagated overnight in 5 ml of synthetic complete media (SD-SCAA) lacking uracil, and supplemented with 2% galactose to induce expression of the GFP-tagged protein constructs. ~10^6 cells were pelleted and the mitochondria stained with Mito-ID Red detection reagent diluted 1:2500 (Mito-ID Red detection kit - Cat# ENZ-51007-500, Enzo Life Sciences, Ann Arbor, MI) according to manufacturer instructions before being affixed to polylysine-coated slides for visualization (Mazia et al., 1975). Mitochondria visualization and protein localization were determined by confocal microscopy with an Olympus Fluoview 1000 Spectral Confocal with a 600x objective (Olympus America, Center Valley, PA). Protein expression was detected via green fluorescence (excitation=488 nm, emission=510 nm) while mitochondria were stained to fluoresce red (excitation=559 nm, emission=598 nm). All samples were visualized at similar gain, PMT voltage, and magnification to directly compare fluorescence levels.

2.4. Enzyme activity assays

All enzyme activity assays were performed on crude lysates generated by disrupting cell pellets resuspended in 500 μL of 50 mM Tris-HCl (pH=7.5) with ~ 100 μL of 0.5mm diameter zirconia/silica beads (BioSpec Products, Bartlesville, OK) in 5×5 s pulses at max speed on a vortexer with the samples maintained on ice for 30 s between pulses. The resulting lysates were clarified by centrifugation before being assayed for either ACD or BCKAD activity. ACD activity was measured in a continuous spectrophotometric assay at 25 °C in a redox reaction described by Izai and coworkers (Izai et al., 1992). ACD oxidizes its substrate isobutyryl-CoA to methacrylyl-CoA, transferring electrons to the intermediate electron carrier phenazine methosulfate (PMS). These electrons are then transferred to the electron acceptor 2, 6-dichlorophenolindophenol (DCPIP) with a simultaneous decrease in absorbance at 600 nm (ε=21 mL mol^{-1} cm^{-1} at pH~8 (McD. Armstrong, 1964). 1 U of activity corresponds to the oxidation of 1 mmol of isobutyryl-CoA/min in the presence of 1 mM N-ethylmaleimide, 0.03 mM isobutyryl-CoA, 1.6 mM PMS, 0.035 mM DCPIP, 0.4 mM FAD^+ and 100 mM potassium phosphate buffer (pH = 8). BCKAD activity was measured spectrophotometrically at 37 °C in an assay first described by Reed and Mukherjee (Reed and Mukherjee, 1969). Reaction progress is monitored by the reduction of NAD^+ at 340 nm. 1 U of activity corresponds to the decarboxylation and oxidation of 1 μmol of 2-oxoisovalerate/min in the presence of 1 mM $MgCl_2$, 0.2 mM thiamine pyrophosphate, 0.2 mM coenzyme A/2 mM dithiothreitol (DTT; Fisher Scientific, Pittsburgh, PA), 2 mM NAD^+, 2 mM L-valine, 4 mM 2-oxoisovalerate and 100 mM potassium phosphate buffer (pH=7). Enzyme activities reported are normalized by total protein levels as measured with a BCA total protein assay (ThermoFisher Scientific, formerly Pierce Biotechnology, Waltham, MA). All reagents from Sigma-Aldrich (St. Louis, MO) unless indicated otherwise.

3. Results and discussion

3.1. Production and mitochondrial targeting of heterologous valine degradation pathway genes

To evaluate the feasibility of isobutanol production via bacterial valine catabolism in yeast, we first needed to sub-clone constructs that could be expressed and localized within yeast. We constructed gene fusions of the first two enzymes (BCKAD and ACD) incorporating an N-terminal *mt* leader peptide and a C-terminal GFP tag for each enzyme to achieve mitochondrial expression and observe its localization. This *mt* leader sequence consisted of the 69 amino acid presequence of the Su9 mitochondrial F_0-ATPase found in *N. crassa* that was previously shown to direct mitochondrial expression in *S. cerevisiae* (Westermann and Neupert, 2000). These constructs were tagged with a S65T mutant of GFP, allowing for rapid and bright visualization of protein expression (Heim et al., 1995). Each gene fusion construct was expressed independently both with and without the *mt* leader peptide to test the ability of yeast to successfully target expression of proteins derived from the prokaryote *Pseudomonas aeruginosa*. We verified the localized expression of these genes by monitoring the green fluorescence of the C-terminal GFP epitope and by mitochondrial staining.

All of the valine degradation gene constructs tested, both with and without the *mt* leader sequence, were readily expressed in *S. cerevisiae* following ~24 h induction with galactose as evidenced by cellular green fluorescence vs. control strains (Fig. 3). In all cases, the presence of the *mt* presequence had a direct impact on the intensity and distribution of green fluorescence throughout the cell. As anticipated, constructs lacking the *mt* leader showed diffuse fluorescence consistent with non-localized expression of these genes within the cytoplasm. This distribution of fluorescence was distinct from the Mito-ID Red mitochondrial staining, which revealed discrete structures that crowd the periphery of the cell. In contrast, the *mt* leader sequence dramatically reduced the amount of fluorescence to localized punctate regions along the cellular margins that generally aligned with mitochondrial staining. That is, the *mt* leader peptide appeared to direct expression towards the mitochondria of the cell. However, this targeted expression dramatically reduced the amount of functional protein as visualized by the reduced green fluorescence, which may be due to the high energy cost involved in translocating proteins across the mitochondrial membranes and their folding within the matrix (Mokranjac and Neupert, 2008; Neupert and Herrmann, 2007). The effects of this energy penalty do not appear to be exclusively correlated with protein size. For instance *acd1*, encoding a 42.6 kDa protein, expresses very strongly in the cytoplasm but weakly in the mitochondria (Fig. 3A) while the slightly larger *lpdV* (48.6 kDa), expresses at comparable levels in both the cytoplasm and mitochondria (Fig. 3E). Despite this penalty, however, mitochondrial expression well above background (Fig. 3F) was observed for each construct with fluorescence approaching roughly half that of the positive mitochondrial fluorescence control (Fig. 3G). These nonlinear effects hint at the complex relationship between compartment environment (e.g. pH, redox potential) and protein expression, and suggests that the mitochondria presents an optimal environment for the proper folding and activity of the valine assimilation pathway.

3.2. Compartmentalization results in higher specific activities of Acd AND bckad

Following the successful targeting of this isobutanol producing candidate pathway to either the mitochondria or the cytoplasm, we measured the total protein activity and assessed the impact of compartmentalization. *acd1* encodes an acyl-CoA dehydrogenase, which belongs to the family of flavin adenine dinucleotide-containing enzymes involved in the β-oxidation of fatty acids and

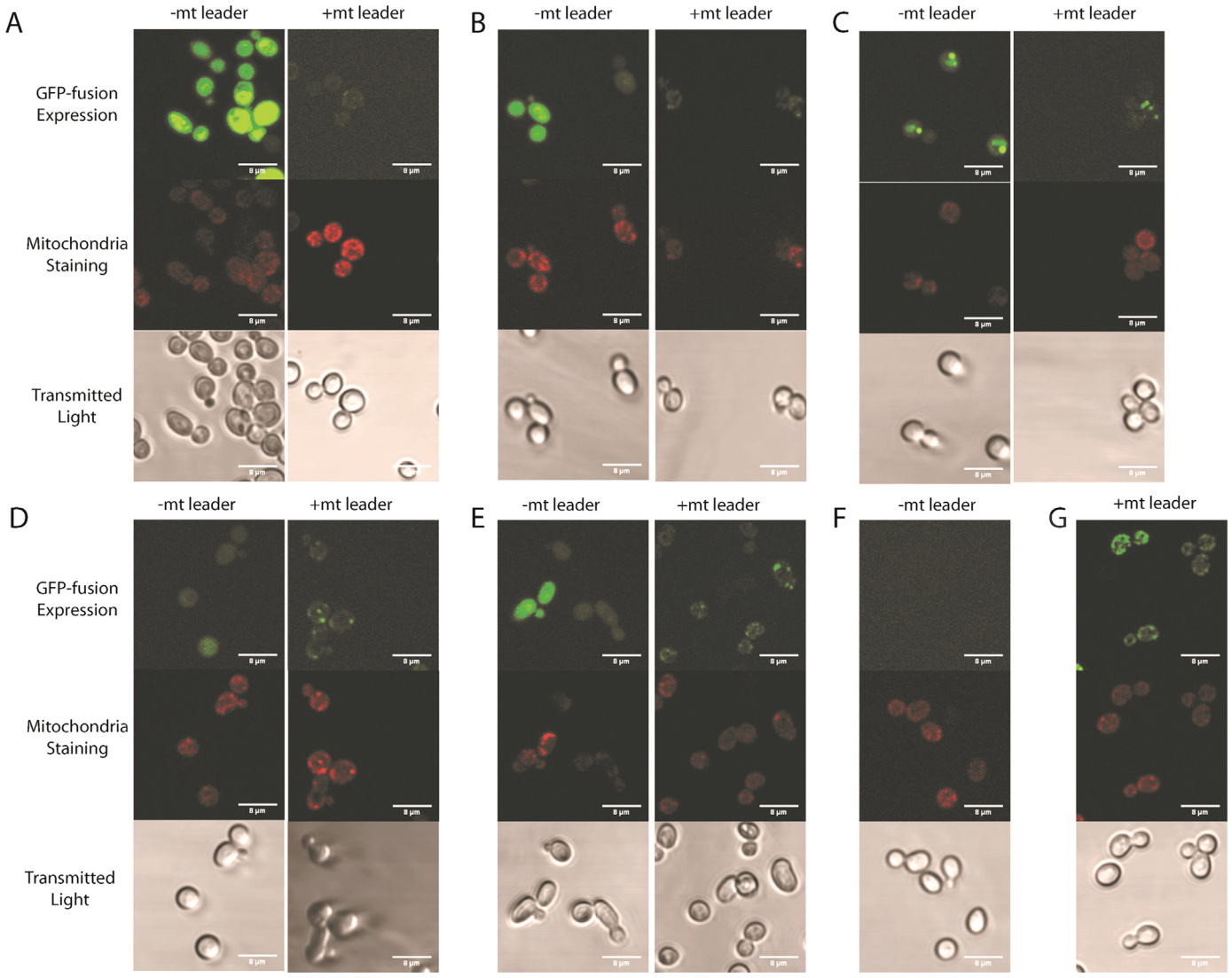

Fig. 3. Valine degradation pathway genes are directed to the yeast mitochondria with the *mt* leader peptide. *S. cerevisiae* CKY263 cells were induced for 24 h with galactose before being stained with the Mito-ID Red kit and visualized by confocal microcopy (Materials and Methods). A) *acd1*; B) *bkdA1*; C) *bkdA2*; D) *bkdB*; E) *lpdV*. F) fluorescence (-) control – *bglA* G) Mitochondrial fluorescence (+) control - *mtGFP*. All images were taken under comparable gain and PMT voltage settings to allow for direct comparison of pixel intensities.

catabolism of many amino acids in many domains of life (Battaile et al., 2002). While the crystal structure for the *P. aeruginosa* ACD is unknown, homologous *acd1* gene products typically form homotetramers or homodimers with the C-terminus forming an α-helix that mediates FAD^+ binding and participates in oligomerization (Djordjevic et al., 1995). Thus, the C-terminal GFP epitope of the cloned *acd1* constructs was anticipated to sterically hinder substrate binding and enzyme assembly, and was removed to evaluate its activity. Similarly, the BCKAD enzyme complex, encoded by *bkdA1*, *bkdA2*, *bkdB*, and *lpdV* forms a complex heteroligomer with octahedral symmetry with as many as 60 subunits (Ævarsson et al., 2000). This large enzyme oxidatively decarboxylates branched short-chain α-ketoacids in a 3-stage reaction and is the first committed step of branched chain amino acid degradation. Given the intricacy of the enzyme complex, we removed the GFP epitope to preserve activity.

We amplified the (mt)*acd1* gene cassettes without the GFP epitope and created constructs that were anticipated to oligomerize to form active ACD (pYES-mtacd/pYES-acd). After 7 h and 24 h of induction and expression in *S. cerevisiae* CKY263 with 2% galactose, cells were harvested, lysed and assayed for activity. Both cytoplasmic and mitochondrial constructs displayed activity above background suggesting routes to carboxylic acid biomonomers from bacterial valine catabolism are potentially feasible. The presence of the *mt* leader peptide was shown to delay expression of functional ACD, possibly due to the energy intensive and dynamic nature of mitochondrial translocation (Fig. 4A). Unlike proteins which are readily translated and folded in the cytoplasm, mitochondrial proteins must be maintained in an unfolded state, actively pumped across the mitochondrial membranes, and then folded correctly and oligomerized (if necessary) before the enzyme is active against substrate (Neupert and Herrmann, 2007). Thus, the nascent energy reserves of early exponential phase may create a bottleneck in translocation, reducing mitochondrial protein activity relative to the cytoplasmic variant at early times as seen in Fig. 4A. However, at 24 h and beyond, activity of mitochondrial ACD surpasses that of its cytoplasmic variant by up to 138% (Fig. 4A). This observation is reproduced in multiple strains (CKY263 and the vacuolar proteases deficient BJ5464), in the presence of multiple plasmids, across vector backbones (pYES vs pRS316), and across induction times (Fig. 4). Experiments performed in triplicate in BJ5464 [p(mt)ACD1 p(mt)BCKAD4 p(mt)

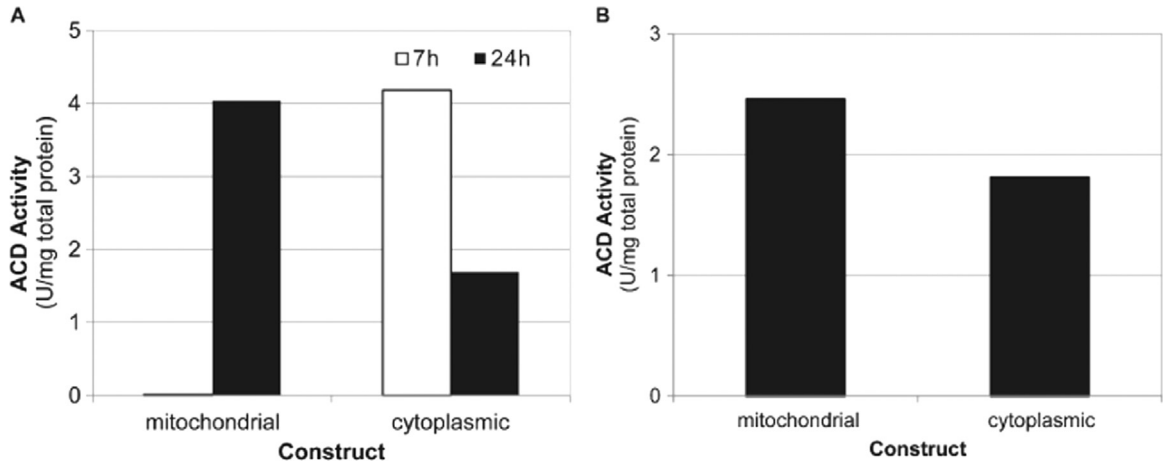

Fig. 4. ACD activity is a function of induction time and cellular compartment. A) Net activity of ACD in *S. cerevisiae* CKY263 lysates expressed from pYES at 7 h and 24 h. B) Net activity of ACD in *S. cerevisiae* BJ5464 expressed from pRS316 [p(mt)ACD1] at 48 h in conjunction with 6 other genes of the valine degradation pathway [p(mt)BCKAD4 and p(mt)CoA]. Net activity is relative to a negative control (mtGFP or empty vector) grown in parallel and normalized against total protein in the crude lysate. 1 U of activity corresponds to the oxidation of 1 mmol of isobutyryl-CoA/min.

CoA2] at 24 h replicate this result with cytoplasmic cultures showing activity indistinguishable from background while mitochondrial cultures display 1.14 ± 0.86 U ACD activity per 10^8 cells. When coupled with the fluorescence data of Fig. 3A, this observation is even more remarkable. Despite the reduced fluorescence and lower expression levels of mitochondrial protein, mitochondrially targeted ACD is more active than cytoplasmic ACD. That is, the specific activity of mitochondrially expressed ACD is higher than cytoplasmic expression variants. This observation is even more striking given the diffuse cytoplasmic expression of this enzyme in its native prokaryotic host. One hypothesis for this behavior is the increased local concentrations of *acd1* monomer and/or substrate (Avalos et al., 2013) stabilize the protein and favor ACD oligomerization leading to a higher specific activity. Moreover, the reduced number of protein degradation pathways within the mitochondria (Käser and Langer, 2000), and abundance of chaperonins, may confer additional protein stability that further improves activity.

Similar experiments with the first committed step of valine catabolism from *P. aeruginosa*, (mt)BCKAD [(mt)*bkdA1,* (mt)*bkdA2*, (mt)*bkdB*, (mt)*lpdV*] show heterologous activity in yeast despite the presence of native homologs (Richard Dickinson, 2000) (Fig. 5). That is, bacterial valine catabolism may be used in yeast to produce precursors for isobutanol and biomonomer production. After 48 h induction in *S. cerevisiae* BJ5464, cytoplasmic and mitochondrial expression of the heterooligomeric BCKAD enzyme complex yield comparable activity. Like ACD, mitochondrial expression of these subunits is dramatically reduced relative to the cytoplasm (Figs. 3B–3E). However, proper folding and assembly of this large oligomeric complex appears to be favored in the mitochondrial matrix leading to comparable total activities, or a higher mitochondrial specific activity. As seen here, heterologous expression in a compartment different from the native host may be more optimal for enzyme specifc activity of an engineered pathway. Future engineering efforts with this pathway are, thus, more likely to be successful by pursuing a mitochondrial-expression approach.

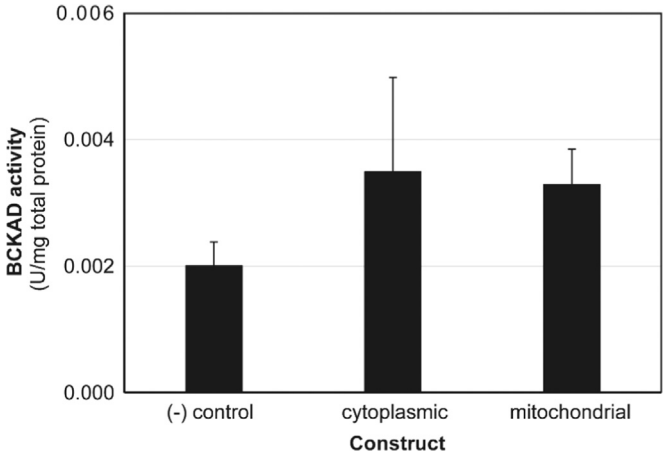

Fig. 5. Total activity of BCKAD does not depend on location of heterologous expression. BCKAD was expressed in *S. cerevisiae* BJ5464 from pRS315 48 h in conjunction with 3 other genes of the valine degradation pathway [p(mt)ACD1 and p(mt)CoA2]. (-) control is empty vector (pRS315). Total activity is relative to a buffer control and normalized against total protein in the crude lysate. 1 U of activity corresponds to the decarboxylation and oxidation of 1 μmol of 2-oxoisovalerate/min.

4. Conclusions

In these studies, we evaluated the feasibility of bacterial valine assimilation in non-pathogenic yeast as an alternate route to monomers and alcohols such as isobutanol, an advanced biofuel. We expressed the first two enzymes of the pathway, BCKAD and ACD, and confirmed that they could be heterologously expressed in yeast and targeted to either the cytoplasm or mitochondria for expression. Although heterologous mitochondrial protein expression was lower than cytoplasmic expression, the total enzyme activity was the same if not greater in the mitochondria. Counterintuitively, the choice of heterologous expression compartment need not be limited by the ones used by the native host as our results demonstrate that non-native environments can improve specific activity. More specifically, the data suggests that the mitochondria is a more optimal environment than the yeast cytosol for folding and assembly of cytoplasmic bacterial valine catabolism. This benefit is likely multiplicative with the increased local enzyme and precursor concentration (Avalos et al., 2013) for future isobutanol and biomonomer production efforts. More broadly, however, our results underscore the importance of the cellular environment in heterologous protein expression and highlights a key parameter to be optimized in recombinant protein expression.

Acknowledgements

We thank Dr. Mary Raven and the NRI-MCDB Microscopy Facility (supported by NIH Grant Number: 1 S10 OD010610-01A1) at UCSB for confocal microscopy assistance. We would also like to thank Prof. Dr. Benedikt Westermann (Universität Bayreuth, Germany) for providing pYES-mtGFP. Funding for this project was provided by the Mitsubishi Chemical Center for Advanced Materials (MC-CAM) at the University of California, Santa Barbara, Project number MRC-NRT-03.

References

Adrio, J.-L., Demain, A.L., 2010. Recombinant organisms for production of industrial products. Bioeng. Bugs 1, 116–131. http://dx.doi.org/10.4161/bbug.1.2.10484.

Ævarsson, A., Chuang, J.L., Max Wynn, R., Turley, S., Chuang, D.T., Hol, W.G., 2000. Crystal structure of human branched-chain α-ketoacid dehydrogenase and the molecular basis of multienzyme complex deficiency in maple syrup urine disease. Structure 8, 277–291. http://dx.doi.org/10.1016/S0969-2126(00)00105-2.

Avalos, J.L., Fink, G.R., Stephanopoulos, G., 2013. Compartmentalization of metabolic pathways in yeast mitochondria improves the production of branched-chain alcohols. Nat. Biotechnol. 31, 335–341. http://dx.doi.org/10.1038/nbt.2509.

Battaile, K.P., Molin-Case, J., Paschke, R., Wang, M., Bennett, D., Vockley, J., Kim, J.-J. P., 2002. Crystal structure of rat short chain Acyl-CoA dehydrogenase complexed with acetoacetyl-CoA comparison with other Acyl-CoA dehydrogenases. J. Biol. Chem. 277, 12200–12207. http://dx.doi.org/10.1074/jbc.M111296200.

Branduardi, P., Longo, V., Berterame, N.M., Rossi, G., Porro, D., 2013. A novel pathway to produce butanol and isobutanol in *Saccharomyces cerevisiae*. Biotechnol. Biofuels 6, 68. http://dx.doi.org/10.1186/1754-6834-6-68.

Daniel Gietz, R., Woods, R.A., 2002. Transformation of yeast by lithium acetate/single-stranded carrier DNA/polyethylene glycol method. In: Fink, C.G., G.R. (Eds.), Methods in Enzymology, Guide to Yeast Genetics and Molecular and Cell Biology - Part B. Academic Press, pp. 87–96.

Demain, A.L., Vaishnav, P., 2009. Production of recombinant proteins by microbes and higher organisms. Biotechnol. Adv. 27, 297–306. http://dx.doi.org/10.1016/j.biotechadv.2009.01.008.

Djordjevic, S., Pace, C.P., Stankovich, M.T., Kim, J.-J.P., 1995. Three-dimensional structure of Butyryl-CoA dehydrogenase from *Megasphaera elsdenii*. Biochemistry 34, 2163–2171. http://dx.doi.org/10.1021/bi00007a009.

Frand, A.R., Kaiser, C.A., 1999. Ero1p oxidizes protein disulfide isomerase in a pathway for disulfide bond formation in the endoplasmic reticulum. Mol. Cell 4, 469–477. http://dx.doi.org/10.1016/S1097-2765(00)80198-7.

Fukuda, H., Casas, A., Batlle, A., 2005. Aminolevulinic acid: from its unique biological function to its star role in photodynamic therapy. Int. J. Biochem. Cell Biol. 37, 272–276. http://dx.doi.org/10.1016/j.biocel.2004.04.018.

Hazelwood, L.A., Daran, J.-M., Maris, A.J.A., van, Pronk, J.T., Dickinson, J.R., 2008. The Ehrlich pathway for fusel alcohol production: a century of research on saccharomyces cerevisiae metabolism. Appl. Environ. Microbiol. 74, 2259–2266. http://dx.doi.org/10.1128/AEM.02625-07.

Heim, R., Cubitt, A.B., Tsien, R.Y., 1995. Improved green fluorescence. Nature 373, 663–664. http://dx.doi.org/10.1038/373663b0.

Hu, J., Dong, L., Outten, C.E., 2008. The redox environment in the mitochondrial intermembrane space is maintained separately from the cytosol and matrix. J. Biol. Chem. 283, 29126–29134. http://dx.doi.org/10.1074/jbc.M803028200.

Ingram, L.O., 1986. Microbial tolerance to alcohols: role of the cell membrane. Trends Biotechnol. 4, 40–44. http://dx.doi.org/10.1016/0167-7799(86)90152-6.

Izai, K., Uchida, Y., Orii, T., Yamamoto, S., Hashimoto, T., 1992. Novel fatty acid beta-oxidation enzymes in rat liver mitochondria. I. Purification and properties of very-long-chain acyl-coenzyme A dehydrogenase. J. Biol. Chem. 267, 1027–1033.

Jones, E.W., 1991. [31] Tackling the protease problem in Saccharomyces cerevisiae. Methods Enzymol., 428–453 (Guide to Yeast Genetics and Molecular Biology. Academic Press).

Käser, M., Langer, T., 2000. Protein degradation in mitochondria. Semin. Cell Dev. Biol. 11, 181–190. http://dx.doi.org/10.1006/scdb.2000.0166.

Kim, D.H., Hwang, I., 2013. Direct targeting of proteins from the cytosol to organelles: the ER versus endosymbiotic organelles. Traffic 14, 613–621. http://dx.doi.org/10.1111/tra.12043.

Knight, T., 2003. Idempotent Vector Design for Standard Assembly of Biobricks. MIT Synth. Biol. Work. Group Tech. Rep. 1721.1/21168.

Kumar, A., Agarwal, S., Heyman, J.A., Matson, S., Heidtman, M., Piccirillo, S., Umansky, L., Drawid, A., Jansen, R., Liu, Y., Cheung, K.-H., Miller, P., Gerstein, M., Roeder, G.S., Snyder, M., 2002. Subcellular localization of the yeast proteome. Genes Dev. 16, 707–719. http://dx.doi.org/10.1101/gad.970902.

Massey, L.K., Sokatch, J.R., Conrad, R.S., 1976. Branched-chain amino acid catabolism in bacteria. Bacteriol. Rev. 40, 42–54.

Mazia, D., Schatten, G., Sale, W., 1975. Adhesion of cells to surfaces coated with polylysine. Applications to electron microscopy. J. Cell Biol. 66, 198–200. http://dx.doi.org/10.1083/jcb.66.1.198.

McD. Armstrong, J., 1964. The molar extinction coefficient of 2,6-dichlorophenol indophenol. Biochim. Biophys. Acta BBA – Gen. Subj. 86, 194–197. http://dx.doi.org/10.1016/0304-4165(64)90180-1.

Mitchell, P., 1961. Coupling of phosphorylation to electron and hydrogen transfer by a chemi-osmotic type of mechanism. Nature 191, 144–148. http://dx.doi.org/10.1038/191144a0.

Mokranjac, D., Neupert, W., 2008. Energetics of protein translocation into mitochondria. Biochim. Biophys. Acta BBA – Bioenerg. 1777, 758–762. http://dx.doi.org/10.1016/j.bbabio.2008.04.009.

Neupert, W., Herrmann, J.M., 2007. Translocation of Proteins into Mitochondria. Annu. Rev. Biochem. 76, 723–749. http://dx.doi.org/10.1146/annurev.biochem.76.052705.163409.

O'Malley, M.A., Theodorou, M.K., Kaiser, C.A., 2012. Evaluating expression and catalytic activity of anaerobic fungal fibrolytic enzymes native to *Piromyces sp.* E2 in Saccharomyces cerevisiae. Environ. Prog. Sustain. Energy 31, 37–46. http://dx.doi.org/10.1002/ep.10614.

Orij, R., Postmus, J., Beek, A.T., Brul, S., Smits, G.J., 2009. In vivo measurement of cytosolic and mitochondrial pH using a pH-sensitive GFP derivative in Saccharomyces cerevisiae reveals a relation between intracellular pH and growth. Microbiology 155, 268–278. http://dx.doi.org/10.1099/mic.0.022038-0.

Paltauf, F., Kohlwein, S.D., Henry, S.A., 1992. 8. Regulation and Compartmentalization of Lipid Synthesis in Yeast, Cold Spring Harbor Monograph Archive, The Molecular and Cellular Biology of the Yeast Saccharomyces. Cold Spring Harbor Laboratory Press, pp. 415–500.

Reed, L.J., Mukherjee, B.B., 1969. [12] α-ketoglutarate dehydrogenase complex from Escherichia coli. Methods Enzymol., 55–61 (Citric Acid Cycle, Academic Press).

Richard Dickinson, J., 2000. Branched-chain keto acid dehydrogenase of yeast. In: John, R.A.H., Sokatch, R.A.H. (Eds.), Methods in Enzymology. Academic Press, pp. 389–398.

Sambrook, J., Russell, D.W., 2001. Molecular cloning: a laboratory manual. CSHL Press.

Sheppard, M.J., Kunjapur, A.M., Wenck, S.J., Prather, K.L.J., 2014. Retro-biosynthetic screening of a modular pathway design achieves selective route for microbial synthesis of 4-methyl-pentanol. Nat. Commun. 5, 5031. http://dx.doi.org/10.1038/ncomms6031.

Sherman, F., 2002. Getting started with yeast. Methods Enzymol., 3–41.

Smith, K.M., Liao, J.C., 2011. An evolutionary strategy for isobutanol production strain development in Escherichia coli. Metab. Eng. 13, 674–681. http://dx.doi.org/10.1016/j.ymben.2011.08.004.

Song, F., Zhuang, Z., Finci, L., Dunaway-Mariano, D., Kniewel, R., Buglino, J.A., Solorzano, V., Wu, J., Lima, C.D., 2006. Structure, function, and mechanism of the phenylacetate pathway hot dog-fold thioesterase paaI. J. Biol. Chem. 281, 11028–11038. http://dx.doi.org/10.1074/jbc.M513896200.

Westermann, B., Neupert, W., 2000. Mitochondria-targeted green fluorescent proteins: convenient tools for the study of organelle biogenesis in *Saccharomyces cerevisiae*. Yeast 16, 1421–1427 10.1002/1097-0061(200011)16:15 < 1421::AID-YEA624 > 3.0.CO;2-U.

Woycechowsky, K.J., Raines, R.T., 2000. Native disulfide bond formation in proteins. Curr. Opin. Chem. Biol. 4, 533.

Zhuang, Z., Song, F., Zhao, H., Li, L., Cao, J., Eisenstein, E., Herzberg, O., Dunaway-Mariano, D., 2008. Divergence of function in the hot dog fold enzyme superfamily: the bacterial thioesterase YciA†. Biochemistry 47, 2789–2796. http://dx.doi.org/10.1021/bi702334h.